Available online at www.sciencedirect.com
SCIENCE DIRECT®
Biochemical and Biophysical Research Communications 336 (2005) 76–83
BBRC
www.elsevier.com/locate/ybbrc

Suppression of expression of muscle-associated proteins by PPARα in brown adipose tissue

Yuhong Tong [a], Atsushi Hara [a,*], Makiko Komatsu [a], Naoki Tanaka [a,b], Yuji Kamijo [a,b], Frank J. Gonzalez [c], Toshifumi Aoyama [a]

[a] Department of Metabolic Regulation, Institute on Aging and Adaptation, Shinshu University Graduate School of Medicine, 3-1-1 Asahi, Matsumoto, Nagano 390-8621, Japan
[b] Department of Internal Medicine, Shinshu University School of Medicine, 3-1-1 Asahi, Matsumoto, Nagano 390-8621, Japan
[c] Laboratory of Metabolism, National Cancer Institute, National Institutes of Health, Bethesda, MD 20892, USA

Received 3 August 2005
Available online 18 August 2005

Abstract

Peroxisome proliferator-activated receptor α (PPARα) belongs to the steroid/nuclear receptor superfamily. Two-dimensional (2D) SDS–PAGE analysis of brown adipose tissue (BAT) unexpectedly revealed six spots that were present only in PPARα-null mice. Proteomic analysis indicated that these proteins were tropomyosin-1 α chain, tropomyosin β chain, myosin regulatory light chain 2, myosin light chain 3, and parvalbumin α. Analyses of mRNA have revealed that PPARα suppressed the genes encoding these proteins in a synchronous manner in adult wild-type mice. Histological and physiological analyses of BAT showed in adult wild-type mice, a marked suppression of BAT growth concurrent with a prominent decrease in lipolytic and thermogenesis activities. These results suggest that in adult mice, PPARα functions to suppress the expression of the proteins that may be involved in the architecture of BAT, and thus may function in keeping BAT in a quiescent state.

Keywords: Peroxisome proliferator-activated receptor α; Brown adipose tissue; Synchronous suppression; Transcriptional regulation; MALDI-TOF MS

Peroxisome proliferator-activated receptor α (PPARα) is a member of nuclear receptors belonging to the steroid hormone receptor superfamily, and mainly exists in the brown adipose tissue (BAT), liver, kidney, and heart, which are characterized by relatively high rates of fatty acid catabolism [1]. It has various functions that are associated with the regulation of lipid transport, storage, and metabolism, and they influence a variety of events in cells [1,2]. The elucidation of PPARα function has been aided by the use of PPARα-null (−/−) mice [3–8]. The present study was performed to determine the influence of PPARα on protein expression in the BAT, liver, kidney, heart, small intestine, serum, and muscle by proteomic analysis. Interestingly, marked differences in the protein expression pattern between PPARα-null (−/−) mice and wild-type (+/+) controls were found only in the BAT. Protein identification by matrix-assisted laser desorption ionization-time-of-flight mass spectrometry (MALDI-TOF MS) and immunoblot analysis, and mRNA analysis were performed. The results revealed a new function for PPARα in BAT.

Materials and methods

Materials and chemicals. Immobiline DryStrips (pH 3–10, 18 cm) were purchased from Amersham Pharmacia Biotechnology (Piscataway, NJ). Montage In-Gel Digest$_{96}$ Kit and ZipTip$_{C18}$ were from

* Corresponding author. Fax: +81 263 37 3094.
E-mail address: kareisei@sch.md.shinshu-u.ac.jp (A. Hara).

0006-291X/$ - see front matter © 2005 Elsevier Inc. All rights reserved.
doi:10.1016/j.bbrc.2005.08.041

Millipore (Bedford, MA). Anti-tropomyosin-1 antibody was from Chemicon International (Temecula, CA). Anti-myosin regulatory light chain (FL-172) and anti-parvalbumin α (T-19) antibodies were from Santa Cruz Biotechnology (Santa Cruz, CA). Alkaline phosphatase-conjugated goat anti-rabbit IgG (H + L) and rabbit anti-goat IgG (H + L) were from Jackson ImmunoResearch Laboratories (West Grove, PA). Adrenocorticotropic hormone (ACTH) fragment 7–38, α-cyano-4-hydroxy cinnamic acid (α-CHCA), and angiotensin I (human) were from Sigma (St. Louis, MO). Iodoacetamide and dithiothreitol (DTT) were from Nacalai Tesque (Kyoto, Japan). 1-Step NBT/BCIP (nitro blue tetrazolium/5-bromo-4-chloro-3-indolylphosphate) was from Pierce (Rockford, IL). [1-^{14}C]Palmitic acid (54 mCi/mmol) was from American Radiolabeled Chemicals (St. Louis, MO). All other reagents were of the highest grade available in Japan.

Animals and experimental treatments. PPARα-null (−/−) mice on an Sv/129 genetic background were produced as described elsewhere [9]. Wild-type (+/+) Sv/129 mice were used as controls in all experiments. In some experiments, 16-week-old mice were fed a diet containing 0.1% (w/w) (4-chloro-6-(2,3-xylidine)-pyrimidinylthio)acetic acid (Wy-14,643) (Chemsyn Science Laboratories) for 2 weeks.

Tissue samples. The BAT was obtained from the symmetrical interscapular regions as follows. Under general anesthesia, the mice were killed by exsanguination via cardiac puncture. The interscapular BAT embedded in the white adipose tissue layer was carefully removed. The BAT thus obtained did not contain any muscle or surrounding tissues. The absence of contamination of other tissues was reconfirmed by two-dimensional (2D) SDS–PAGE later (data not shown). Liver, kidney, heart, small intestine, and muscle were then removed, and each tissue was weighed and stored at −80 °C until analysis.

2D SDS–PAGE. Each tissue was homogenized in a gel-swelling reagent containing urea, DTT, Pharmalyte 3–10, acetic acid, Orange G, and Triton X-100 [10]. Then the supernatant was obtained by centrifugation (15,200*g*, 30 min) at 4 °C and used for 2D SDS–PAGE. In brief, the protein samples obtained from 5 to 20 mg tissue were loaded on a re-swollen Immobiline DryStrip, respectively. Then, the isoelectric focusing was carried out at 20 °C. After the gel strips were equilibrated with the SDS-treatment solution, the proteins were separated by SDS–PAGE using 200 mM Tris–HCl (pH 8.8) for anodic electrode buffer and 100 mM Tris–Tricine for cathodic electrode buffer at 30 mA for 4 h at 20 °C. The samples of PPARα-null (−/−) mice and wild-type (+/+) controls were simultaneously analyzed in the same apparatus [10,11].

In-gel digestion. Individual protein spots separated by 2D SDS–PAGE were excised from the gel after staining with Coomassie brilliant blue R-250 and digested using Montage In-Gel Digest$_{96}$ Kit based on the methods according to the manufacturer's protocol (http://www.millipore.com/userguides.nsf/docs/P36379). Briefly, the protein embedded in the gel was digested overnight at 30 °C using trypsin in ammonium bicarbonate buffer. Peptides were extracted from the gels with trifluoroacetic acid-containing acetonitrile and purified with ZipTip$_{C18}$. Finally, the purified peptides were analyzed with α-CHCA by MALDI-TOF MS as follows.

MALDI-TOF MS. A Voyager Elite XL Biospectrometry workstation (PerSeptive Biosystem, Framingham, MA) equipped with a delayed extraction ion source was used for MALDI-TOF MS analysis in the reflector mode with the following parameters: accelerating voltage, 22 kV; grid voltage, 80% of the accelerating voltage; guide wire voltage, 0.05% of the accelerating voltage; delay time, 200 ns. A nitrogen laser (337 nm) was used for ionization. The calibration was performed with the monoisotopic peaks of the dimer of α-CHCA (379.0930 m/z), angiotensin I (1296.6853 m/z), and ACTH (7-38 clip) (3657.9294 m/z).

Database searching. Peptide mass data from MALDI-TOF MS were subjected to a database search using MS-Fit, a typical peptide mass fingerprinting program on the web site of the University of California, San Francisco (http://prospector.ucsf.edu/).

Immunoblot analysis. Immunoblot analysis was performed as described previously [3]. Protein samples obtained from the BAT were subjected to 2D SDS–PAGE as above and the separated proteins were transferred to nitrocellulose membranes in the blotting buffer containing 5% (v/v) methanol at 12 V for 1 h. After blotting, the membranes were sequentially incubated with the primary antibody, followed by alkaline phosphatase-conjugated secondary antibody. The primary antibodies used were rabbit polyclonal antibody against tropomyosin-1 and myosin regulatory light chain, and goat polyclonal antibody against parvalbumin α. Rabbit polyclonal antibodies against medium chain acyl-CoA dehydrogenase (MCAD) [12], very long chain acyl-CoA dehydrogenase (VLCAD) [13], long chain acyl-CoA dehydrogenase (LCAD) [12], and carnitine palmitoyl-CoA transferase II (CPT II) [14] were also used as primary antibodies. The positive immunoreactive spots were visualized by staining with NBT/BCIP.

Analysis of mRNA. Analysis of mRNA was performed by Northern blotting as previously described [3]. Total RNA from the BAT was extracted, electrophoresed on 1.1 M formaldehyde-containing 1% (w/v) agarose gels, and transferred to nylon membranes. The membranes were incubated with ^{32}P-labeled cDNA probes and analyzed on a Fuji system analyzer (Fuji Photo Film, Tokyo, Japan). The cDNA probes were synthesized by reverse transcriptase PCR (RT-PCR). Primer sequences were as follows: for tropomyosin-1 α chain (GenBank Accession No. X64831), 5′-agatgagctggtgtcactgc-3′ and 5′-cggcacatttgccttctgag-3′; for tropomyosin β chain (X12650), 5′-cgaggtggaaaagtattccg-3′ and 5′-tctcc tccagaagtttgatc-3′; for myosin regulatory light chain 2 (NM_016754), 5′-atctaagacatggcacccaa-3′ and 5′-acgtagcagatgttcttgta-3′; for myosin light chain 3 (K02238, K02239, and K02240), 5′-agtgctgaccagattgccga-3′ and 5′-cgattttcttagcattcatc-3′; for parvalbumin α (X54613), 5′-aagaaggcgata ggagcctt-3′ and 5′-ttcaaccccaatcttgccgt-3′; for PPARα (NM_011144), 5′-cagagcaaccatccagatga-3′ and 5′-aaacgcaacgtagagtgctg-3′; for MCAD (NM_007382), 5′-tgcttttgatagaaccagacctacagt-3′ and 5′-attgtccaaaag ccaaacctatcta-3′; for VLCAD (NM_017366), 5′-aaaatcttttgctcggaggc-3′ and 5′-aatccctttcttgtgtttca-3′; for uncoupling protein-1 (UCP-1) (NM_009463), 5′-ctgcctctctcggaaacaag-3′ and 5′-cagaaaagaagccacaa acc-3′; for peroxisome proliferator-activated receptor γ coactivator-1 (PGC-1) (NM_008904), 5′-attttgatagtttactgaag-3′ and 5′-ctcacatgtgtaca tatgta-3′.

Morphological analysis. Small sections of the BAT from each mouse were fixed in 10% buffered formalin, and the sections were stained with hematoxylin and eosin (H&E) as described earlier [4].

Triglyceride determination. Triglyceride concentrations were measured using a kit purchased from Wako (Osaka, Japan) based on the methods according to the manufacturer's protocol.

Palmitic acid β-oxidation activity. Fatty acid β-oxidation activity was measured as follows [15]. Briefly, the BAT was homogenized in four volumes of 0.25 M sucrose containing 1 mM EDTA. Homogenate was incubated with the assay medium containing 50 μM [1-^{14}C]palmitic acid. Radioactive degradation products were counted after removal of unreacted substrate.

Results

Six intense spots were detected in the pattern of BAT proteins from PPARα-null (−/−) mice by 2D SDS–PAGE analysis

The proteins of the interscapular BAT, liver, kidney, heart, small intestine, serum, and muscle obtained from PPARα-null (−/−) and wild-type (+/+) mice were analyzed using 2D SDS–PAGE, respectively. No notable differences were found in any of the tissues examined in PPARα-null (−/−) and wild-type (+/+) mice, with

the exception of BAT. Six intense spots were detected in the pattern of BAT proteins from PPARα-null (−/−) mice as compared with those from wild-type (+/+) controls (Fig. 1).

Protein identification by MALDI-TOF MS and immunoblot analysis

Spots 1–6 were analyzed by MALDI-TOF MS after digestion with trypsin, respectively. The mass spectra of peptides obtained from these spots are shown in Fig. 2. The peptide pattern obtained from each spot was subjected to a database analysis using MS-Fit and the following proteins were identified. Spot 1, parvalbumin α (Swiss-Prot, P32848); spots 2 and 3, myosin regulatory light chain 2 (Swiss-Prot, P97457); spot 4, myosin light chain 3 (Swiss-Prot, P05978); spot 5, tropomyosin-1 α chain (Swiss-Prot, P58771); and spot 6, tropomyosin β chain (Swiss-Prot, P58774). For spots 2 and 3, identical identification results were obtained by analysis using MS-Fit. The difference in mobility of these two spots on SDS–PAGE indicated that the p*I* values may differ, although no further analyses were performed. About 70–90% of the total tryptic peptides obtained from each spot corresponded to the database by MS-Fit analysis. To confirm these results, immunoblot analyses were performed. Spot 1, spots 2 and 3, and spot 5 were specifically stained with anti-parvalbumin α, anti-myosin regulatory light chain, and anti-tropomyosin-1 antibodies, respectively, although only very faint spots which were thought to be non-specific were visible (data not shown). Surprisingly, the proteins found in spots 1–6 are known to exist mainly in the muscle [16].

Analysis of mRNA

To confirm the expression of the five proteins in PPARα-null (−/−) mice, Northern blot analysis was carried out. After the resulting data were subjected to densitometric and statistical analyses, the typical patterns are shown in Fig. 3. The contents of all five mRNAs in the BAT from 16-week-old PPARα-null (−/−) mice were about 7.0-fold of wild-type (+/+) controls. These results were compatible with the observation that the expression levels of these five proteins in the BAT from wild-type (+/+) mice were not expressed to any appreciable degree (Fig. 1). These observations also suggested that the suppression of expression associated with PPARα occurred at the transcription level, although we cannot exclude any influence on protein stabilization. The mRNA contents of PPARα (3.5-fold of 16-week-old control), MCAD (4.0-fold), VLCAD (3.0-fold), and UCP-1 (1.8-fold) increased in Wy-14,643-treated wild-type (+/+) mice but not in PPARα (−/−) mice. Since MCAD, VLCAD, and UCP-1 are known target genes of PPARα [3,17], these data confirmed that PPARα activation occurred in the BAT. However, the contents of the mRNAs encoding all the five proteins in Wy-14,643-treated wild-type (+/+) mice decreased to less than half of the constitutive levels. On the other hand, induction of MCAD, VLCAD, and UCP-1 by Wy-14,643 was not observed in the BAT from PPARα-null (−/−) mice, and the contents of the mRNAs encoding all the five proteins in Wy-14,643-treated PPARα-null (−/−) mice were similar to the control levels. These results indicated that transcriptional suppression of these five proteins occurred in a synchro-

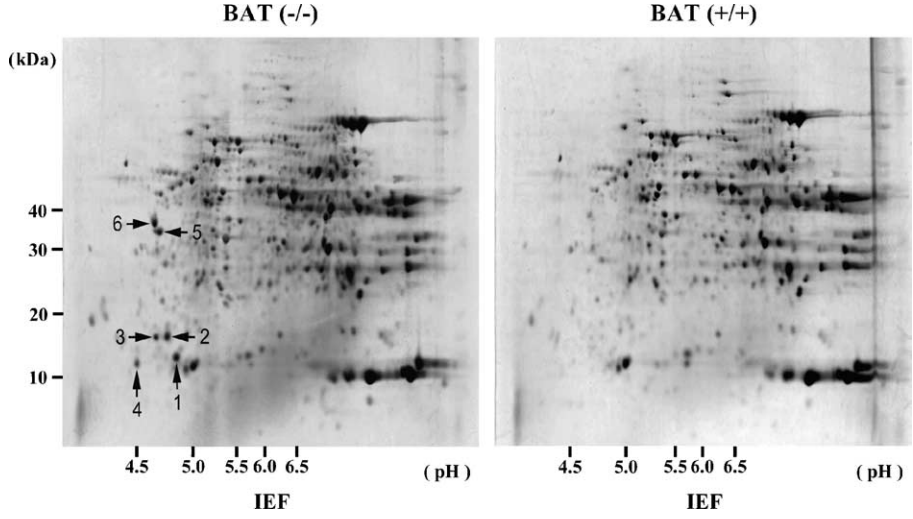

Fig. 1. SDS–PAGE analysis of BAT obtained from PPARα-null (−/−) and wild-type (+/+) mice. The protein samples obtained from 20 mg interscapular BAT were loaded on a re-swollen Immobiline DryStrip, respectively. The proteins were separated by IEF, followed by 2D SDS–PAGE. The samples of PPARα-null (−/−) mice and wild-type (+/+) controls were simultaneously analyzed in the same apparatus. The spots numbered from 1 to 6 are indicated by arrows on the left gel. kDa, kilodalton; IEF, isoelectric focusing.

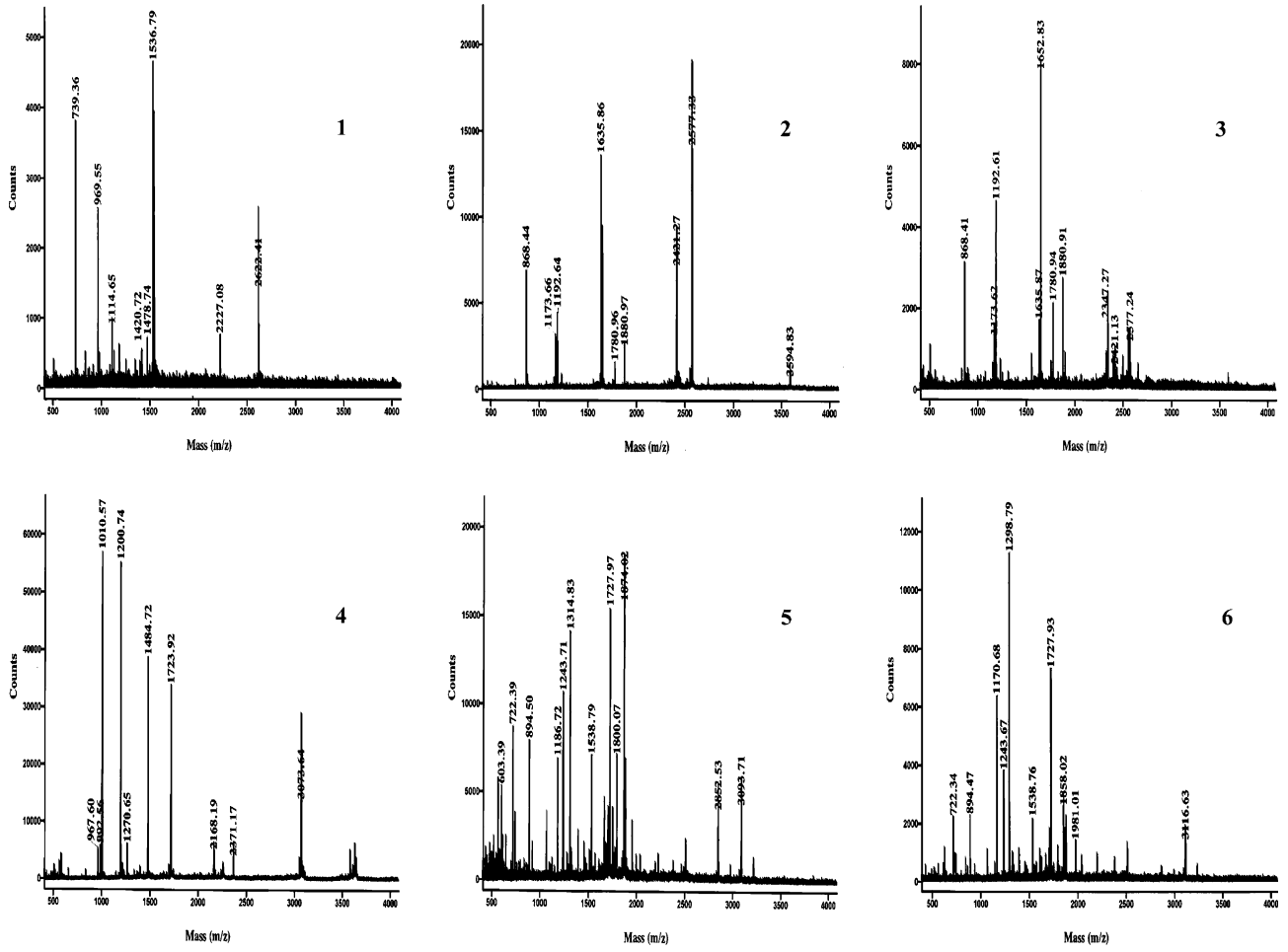

Fig. 2. MALDI-TOF MS spectra of the tryptic peptides obtained from six protein spots. Interscapular BAT of PPARα-null (−/−) mice were analyzed by 2D SDS–PAGE as shown in Fig. 1, and protein spots 1–6 were excised and digested overnight at 30 °C using Montage In-Gel $Digest_{96}$ Kit containing trypsin, respectively. Peptides were extracted from the gels and purified with $ZipTip_{C18}$. Finally, the purified peptides were eluted from $ZipTip_{C18}$ and analyzed by MALDI-TOF MS in the reflector mode. The numbers on each peak top indicate the molecular mass. The number of each spectrum corresponds to spots 1–6 in the left gel of Fig. 1.

nous manner through PPARα, and that this suppression was increased by PPARα activation. It is well known that BAT grows quickly after birth (growth stage) to adopt themselves to circumstance by keeping their body temperature through heat production. To examine the physiological significance of the transcriptional regulation of these five proteins in the BAT, mRNA levels were further compared using the BAT taken from 3-day-old (new born infant), 3-week-old (growth stage of BAT), and 16-week-old mice (quiescent stage of BAT). A PPARα-independent increase was observed in the mRNAs encoding these five proteins in the BAT at 3 weeks after birth in both mouse strains (7- to 12-fold of 3-day-old controls). The content of PPARα mRNA in the BAT at 3 weeks after birth was higher than that in the other two stages. PPARα-independent and transcriptional activation of MCAD (7-fold of 3-day-old controls), VLCAD (8-fold), UCP-1 (4-fold), and PGC-1 (5-fold) was also observed in the BAT at 3 weeks after birth. The transcriptional activation of MCAD and VLCAD, and that of UCP-1 and PGC-1 suggested an increase in lipolytic activity and enhanced thermogenesis at this stage, respectively. On the other hand, these activities in the BAT from adult wild-type (+/+) mice at 16 weeks after birth returned to steady-state level, indicating that the BAT of adult mice was in a quiescent state where production of heat by BAT became relatively low level as shown below.

Characterization of BAT in growth and lipolytic ability

To understand the significance of synchronous regulation in the expression of the five proteins, BAT samples under the four conditions used were further characterized. In a preliminary experiment, during the first 4 weeks of development, BAT was found to grow more rapidly. After 4 weeks, the BAT weight was maintained at constant levels (data not shown). The ratio of BAT weight/body weight at 3 weeks after birth (0.5%) was much higher than those in the other stages in both

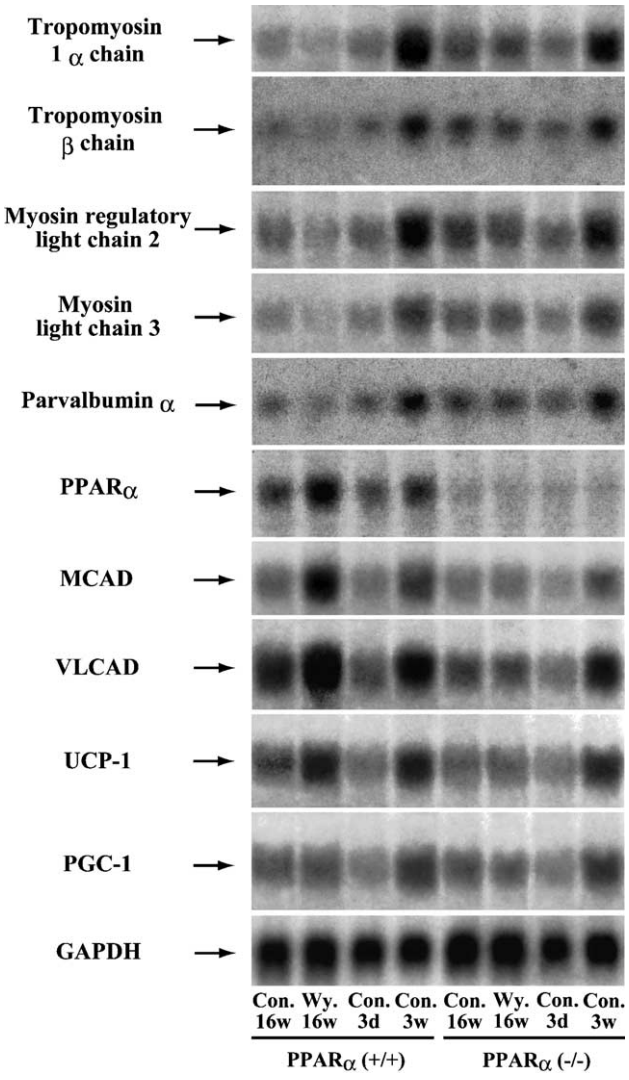

Fig. 3. Northern blot analysis of the BAT. Total RNA from the BAT was extracted, electrophoresed on 1.1 M formaldehyde-containing 1% (w/v) agarose gels, and transferred to nylon membranes. The membranes were incubated with ^{32}P-labeled cDNA probes and analyzed on a Fuji system analyzer. Five micrograms of total RNA was used, respectively. The cDNA probes used were for tropomyosin-1 α chain, tropomyosin β chain, myosin regulatory light chain 2, myosin light chain 3, parvalbumin α, PPARα, MCAD, VLCAD, UCP-1, PGC-1, and glyceraldehyde-3-phosphate dehydrogenase (GAPDH). Then, the resulting data were subjected to densitometric and statistical analyses. Con., control; Wy., Wy-14,643; 16w, 16-week-old; 3w, 3-week-old.

mouse strains (0.2%), suggesting that the BAT at 3 weeks after birth in both mouse strains was in the growth stage and was involved in highly active thermogenesis. At 16 weeks after birth, the ratio dropped to a constant level (0.2%), suggesting that the BAT at 16 weeks after birth was in a quiescent stage. On the other hand, histological analysis with H&E staining demonstrated slight, moderate, and very heavy accumulation of lipid droplets in the BAT at 3 days, 3 weeks, and 16 weeks after birth, respectively, in both mouse strains. The administration of Wy-14,643, a potent PPARα agonist, caused a marked reduction in lipid droplets in wild-type (+/+) mice as compared with PPARα-null (−/−) mice (Fig. 4A). Analyses of triglyceride contents confirmed these histological data, which revealed about 40, 90, and 220 mg triglyceride/g tissue in the BAT at 3 days, 3 weeks, and 16 weeks after birth, respectively, in both mouse strains (Fig. 4B). The lipolytic ability was then examined by determining the changes in triglyceride accumulation. Palmitic acid β-oxidation's overall activity was very low (25 pmol/min/mg protein), high (221 pmol/min/mg protein), and moderate (89 pmol/min/mg protein) in the BAT at 3 days, 3 weeks, and 16 weeks after birth, respectively, in wild-type (+/+) mice (Fig. 4C). The activities in PPARα-null (−/−) mice showed similar tendency to those in wild-type (+/+) mice, although the former activity levels were 50–60% of the latter. The administration of Wy-14,643 caused a 3.0-fold increase in palmitic acid β-oxidation in wild-type (+/+) mice and almost no increase in PPARα-null (−/−) mice. These data were consistent with those from mRNA analyses (MCAD, VLCAD) (Fig. 3). The low lipolytic activities in the BAT at 16 weeks after birth in both mouse strains probably contribute to both the low activities of thermogenesis and the intensive triglyceride accumulation.

Discussion

The results of the present study unexpectedly showed that five proteins that existed in trace amounts in the BAT of adult wild-type (+/+) mice were intensively expressed in a synchronous manner in the BAT of adult PPARα-null (−/−) mice. Proteomic analyses indicated that these five proteins were tropomyosin-1 α chain, tropomyosin β chain, myosin regulatory light chain 2, myosin light chain 3, and parvalbumin α, respectively. Although these proteins are generally associated with muscle, it was confirmed that they were expressed and regulated in the BAT. Their expression was co-ordinately suppressed through a PPARα-dependent mechanism and this suppression was enhanced by ligand activation of PPARα. As the transcriptional suppression occurred in a synchronous manner, it was presumed that a specific regulatory region might exist upstream of each of the genes encoding these proteins. A direct involvement of PPARα in this expression however is not known. It is likely that the influence of PPARα is indirect possible by altering the activity of other transcription factors.

Although these five proteins are known to have important roles in muscle contraction, the data presented in this study suggest that they play important roles in the BAT. The BAT cells, differing from white adipose tissue cells, have very complex and specific membrane structures as described below. These cells come into such close contact with a rich network of capillaries that the

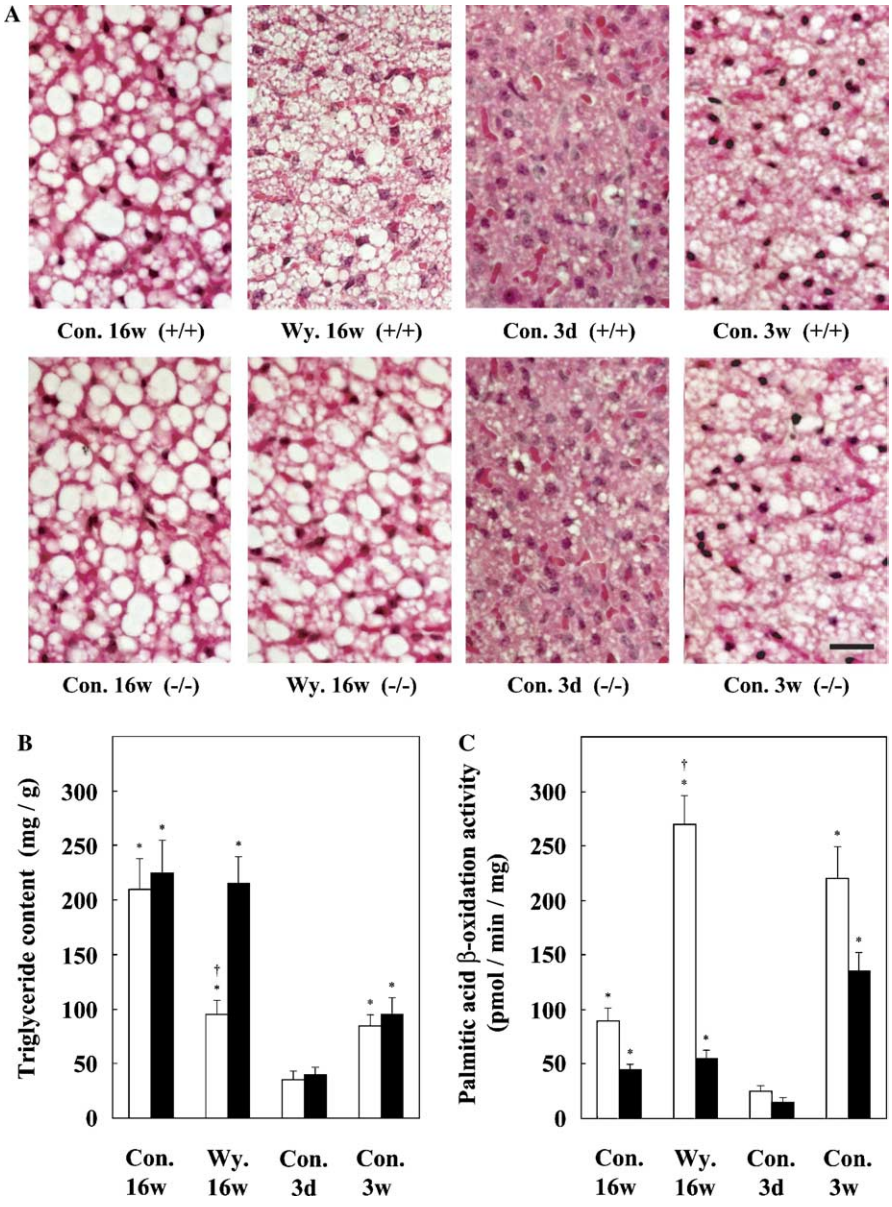

Fig. 4. Histological and biochemical analyses of the BAT. (A) Small sections of the BAT from each mouse were fixed in 10% buffered formalin, and the sections were stained with H&E. Scale bar on the lower right corner of the lower right photograph, 20 μm. Triglyceride contents (B) and palmitic acid β-oxidation activities (C). The contents and activities in the BAT of 3-day-old, 3-week-old, and 16-week-old mice with or without feeding a diet containing 0.1% (w/w) Wy-14,643 for 2 weeks were measured, respectively. Triglyceride concentrations were measured using a kit based on the methods according to the manufacturer's protocol. Fatty acid β-oxidation activity was measured as follows: BAT was homogenized in four volumes of 0.25 M sucrose containing 1 mM EDTA. The homogenate was incubated with the assay medium containing 50 μM [1-^{14}C]palmitic acid. Radioactive degradation products were counted after the removal of unreacted substrate. White and black bars indicate control wild-type (+/+) and PPARα-null (−/−) mice, respectively. Values are presented as means ± SD ($n = 5$). *$P < 0.01$ in the comparison with 3-day-old control mice, respectively; $^{\dagger}P < 0.01$ in the comparison with 16-week-old wild-type (+/+) controls. Significant differences ($P < 0.01$) between wild-type (+/+) and PPARα-null (−/−) mice at each condition were ascertained in (C).

heat generated can be easily transmitted into the bloodstream [18]. Lipid is accumulated in numerous and small lipid droplets in the BAT cells [18]. The BAT cells have a complex membrane structure with a very large number of mitochondria [18]. In lipolysis, cytoplasmic microtubules, a component of the cytoskeleton, arrange the lipid droplets in a radial pattern and thus enhance the transport efficiency of lipids [19]. Of the proteins identified in the present study, tropomyosin is known to associate with microfilaments, also a component of the cytoskeleton, in preadipocytes. Thus, tropomyosin affects cell adhesion and thereby cell shape during adipocyte differentiation [20]. Myosin regulatory light chain and myosin light chain are cytoskeletal proteins and have been reported to be present widely in non-muscle tissues in addition to muscle [21,22]. Parvalbumin is known to

exist in the mitochondria or microtubules of the testis [23], and it has also been shown to interact with other structural components of the cytoskeleton [24,25]. In BAT, however, there have been no reports concerning the five proteins found in this study. Thus, it is assumed that these proteins play important roles in BAT cells by virtue of their involvement in the construction and maintenance of the cytoskeleton and membrane structure. Additionally, a large amount of these proteins seems to be required particularly in the growth stage of BAT, as shown in Results.

In this study, the results derived from the following three conditions used provided important information, which led to clues on the transcriptional regulation of these five proteins. During the growth stage of BAT such as 3 weeks after birth, both the lipolytic and thermogenesis activities increased in a PPARα-independent manner, which was probably associated with limited levels of lipid accumulation. BAT growth was increased in both mouse strains, which was compatible with the possible transcriptional activation of these five proteins. These developmental changes may be caused by the actions of hitherto unknown factors to keep body temperature by production of heat. During the steady-state stage of BAT such as 16 weeks after birth, lipolytic and thermogenesis activities were decreased when comparing with those in the growth stage, due perhaps to heavy lipid accumulation. BAT growth was suppressed in both mouse strains, which probably affected expression levels of these five proteins. Indeed, the expression levels of these five proteins were very low in wild-type (+/+) mice and considerably higher in PPARα-null (−/−) mice, which suggests that the expression is suppressed either directly or indirectly by PPARα in a synchronous manner when BAT growth is limited. In the BAT of Wy-14,643-treated wild-type (+/+) mice, both lipolytic and thermogenesis abilities increased, which was consistent with a significant decrease in lipid accumulation. BAT weight remained unchanged, which was compatible with the PPARα-dependent suppression of these five proteins.

Taken together, we propose a novel function of PPARα in suppressing the expression of at least five proteins when BAT growth becomes low level in adult mice, and this activity is enhanced by PPARα ligand. At present, the precise role of these proteins in BAT is not known, but it is tempting to speculate that they are involved in the physiology of this tissue. One possibility is that the decreases of these through PPARα may function in keeping BAT in a quiescent state in adult mice. Although expression levels of numerous other proteins may be suppressed rationally during the steady-state stage of BAT, the presence of the PPARα-dependent synchronous suppression in this study should be novel and important physiologically, and will contribute to understand the regulation mechanisms of protein expression in the organs under steady-state stage.

The molecular mechanism of the activation of the muscle-related genes remains a mystery. Further studies are required to establish whether PPARα directly interacts with the promoter of these genes or interferes with positive transactivation by other nuclear receptors, transcription factors or co-activators.

Finally, as the detection of protein spots by 2D SDS–PAGE used in the present study has relatively low resolution and only detects the most abundant proteins, future studies using DNA microarray analysis may yield additional genes that are subjected to PPARα-dependent transcriptional suppression in BAT or other tissues. The results of the present study will provide useful information to further understand the mechanism of adult BAT reactivation by cold acclimatization [26].

Acknowledgment

This work was supported in part by President's Discretionary Fund from the President of Shinshu University.

References

[1] B. Desvergne, W. Wahli, Peroxisome proliferator-activated receptors: nuclear control of metabolism, Endocr. Rev. 20 (1999) 649–688.
[2] S. Mandard, M. Müller, S. Kersten, Peroxisome proliferator-activated receptor α target genes, Cell. Mol. Life Sci. 61 (2004) 393–416.
[3] T. Aoyama, J.M. Peters, N. Iritani, T. Nakajima, K. Furihata, T. Hashimoto, F.J. Gonzalez, Altered constitutive expression of fatty acid-metabolizing enzymes in mice lacking the peroxisome proliferator-activated receptor α (PPARα), J. Biol. Chem. 273 (1998) 5678–5684.
[4] K. Watanabe, H. Fujii, T. Takahashi, M. Kodama, Y. Aizawa, Y. Ohta, T. Ono, G. Hasegawa, M. Naito, T. Nakajima, Y. Kamijo, F.J. Gonzalez, T. Aoyama, Constitutive regulation of cardiac fatty acid metabolism through peroxisome proliferator-activated receptor α associated with age-dependent cardiac toxicity, J. Biol. Chem. 275 (2000) 22293–22299.
[5] Y. Kamijo, K. Hora, N. Tanaka, N. Usuda, K. Kiyosawa, T. Nakajima, F.J. Gonzalez, T. Aoyama, Identification of functions of peroxisome proliferator-activated receptor α in proximal tubules, J. Am. Soc. Nephrol. 13 (2002) 1691–1702.
[6] N. Tanaka, K. Hora, H. Makishima, Y. Kamijo, K. Kiyosawa, F.J. Gonzalez, T. Aoyama, In vivo stabilization of nuclear retinoid X receptor α in the presence of peroxisome proliferator-activated receptor α, FEBS Lett. 543 (2003) 120–124.
[7] J.M. Peters, T. Aoyama, R.C. Cattley, U. Nobumitsu, T. Hashimoto, F.J. Gonzalez, Role of peroxisome proliferator-activated receptor α in altered cell cycle regulation in mouse liver, Carcinogenesis 19 (1998) 1989–1994.
[8] T. Nakajima, Y. Kamijo, N. Tanaka, E. Sugiyama, E. Tanaka, K. Kiyosawa, Y. Fukushima, J.M. Peters, F.J. Gonzalez, T. Aoyama, Peroxisome proliferator-activated receptor α protects against alcohol-induced liver damage, Hepatology 40 (2004) 972–980.
[9] S.S. Lee, T. Pineau, J. Drago, E.J. Lee, J.W. Owens, D.L. Kroetz, P.M. Fernandez-Salguero, H. Westphal, F.J. Gonzalez, Targeted disruption of the α isoform of the peroxisome proliferator-

activated receptor gene in mice results in abolishment of the pleiotropic effects of peroxisome proliferators, Mol. Cell. Biol. 15 (1995) 3012–3022.
[10] T. Toda, Current status and perspectives of proteomics in aging research, Exp. Gerontol. 35 (2000) 803–810.
[11] P.H. O'Farrell, High resolution two-dimensional electrophoresis of proteins, J. Biol. Chem. 250 (1975) 4007–4021.
[12] S. Furuta, S. Miyazawa, T. Hashimoto, Purification and properties of rat liver acyl-CoA dehydrogenases and electron transfer flavoprotein, J. Biochem. (Tokyo) 90 (1981) 1739–1750.
[13] K. Izai, Y. Uchida, T. Orii, S. Yamamoto, T. Hashimoto, Novel fatty acid β-oxidation enzymes in rat liver mitochondria. I. Purification and properties of very-long-chain acyl-coenzyme A dehydrogenase, J. Biol. Chem. 267 (1992) 1027–1033.
[14] S. Miyazawa, H. Ozasa, T. Osumi, T. Hashimoto, Purification and properties of carnitine octanoyltransferase and carnitine palmitoyltransferase from rat liver, J. Biochem. (Tokyo) 94 (1983) 529–542.
[15] Y. Shindo, T. Osumi, T. Hashimoto, Effects of administration of di-(2-ethylhexyl)phthalate on rat liver mitochondria, Biochem. Pharmacol. 27 (1978) 2683–2688.
[16] J.C. Sanchez, D. Chiappe, V. Converset, C. Hoogland, P.A. Binz, S. Paesano, R.D. Appel, S. Wang, M. Sennitt, A. Nolan, M.A. Cawthorne, D.F. Hochstrasser, The mouse SWISS-2D PAGE database: a tool for proteomics study of diabetes and obesity, Proteomics 1 (2001) 136–163.
[17] M.J. Barberá, A. Schlüter, N. Pedraza, R. Iglesias, F. Villarroya, M. Giralt, Peroxisome proliferator-activated receptor α activates transcription of the brown fat uncoupling protein-1 gene. A link between regulation of the thermogenic and lipid oxidation pathways in the brown fat cell, J. Biol. Chem. 276 (2001) 1486–1493.
[18] B. Young, J.W. Heath, Wheater's Functional Histology: A Text and Colour Atlas, fourth ed., Churchill Livingstone, London, 2000, pp. 65–79.
[19] H. Sugihara, N. Yonemitsu, K. Ohta, S. Miyabara, A. Nagayama, Immunocytochemistry of the microtubules of fat-laden cells. Brown fat cells and adrenocortical cells in primary monolayer culture, Histochemistry 79 (1983) 227–236.
[20] J.L. Rodriguez Fernandez, A. Ben-Ze'ev, Regulation of fibronectin, integrin and cytoskeleton expression in differentiating adipocytes: inhibition by extracellular matrix and polylysine, Differentiation 42 (1989) 65–74.
[21] J. Kolega, S. Kumar, Regulatory light chain phosphorylation and the assembly of myosin II into the cytoskeleton of microcapillary endothelial cells, Cell Motil. Cytoskeleton 43 (1999) 255–268.
[22] M. Schleicher, B. André, C. Andréoli, L. Eichinger, M. Haugwitz, A. Hofmann, J. Karakesisoglou, M. Stöckelhuber, A.A. Noegel, Structure/function studies on cytoskeletal proteins in *Dictyostelium* amoebae as a paradigm, FEBS Lett. 369 (1995) 38–42.
[23] H. Fritz-Niggli, C. Nievergelt-Egido, C.W. Heizmann, Calcium-binding parvalbumin in *Drosophila* testis in connection with in vivo irradiation, Radiat. Environ. Biophys. 27 (1988) 59–65.
[24] A. De Haas Ratzliff, I. Soltesz, Differential expression of cytoskeletal proteins in the dendrites of parvalbumin-positive interneurons versus granule cells in the adult rat dentate gyrus, Hippocampus 10 (2000) 162–168.
[25] C.C. Stichel, W. Singer, C.W. Heizmann, A.W. Norman, Immunohistochemical localization of calcium-binding proteins, parvalbumin and calbindin-D 28k, in the adult and developing visual cortex of cats: a light and electron microscopic study, J. Comp. Neurol. 262 (1987) 563–577.
[26] P. Puigserver, Z. Wu, C.W. Park, R. Graves, M. Wright, B.M. Spiegelman, A cold-inducible coactivator of nuclear receptors linked to adaptive thermogenesis, Cell 92 (1998) 829–839.